

# Pressure effects on the magnetic susceptibility of $\text{FeTe}_x$ ( $x \simeq 1.0$ )

A V Fedorchenko<sup>1</sup>, G E Grechnev<sup>1</sup>, V A Desnenko<sup>1</sup>, A S Panfilov<sup>1</sup>,  
S L Gnatchenko<sup>1</sup>, V Tsurkan<sup>2,3</sup>, J Deisenhofer<sup>2</sup>, A Loidl<sup>2</sup>,  
O S Volkova<sup>4</sup> and A N Vasiliev<sup>4</sup>

<sup>1</sup> B Verkin Institute for Low Temperature Physics and Engineering, National Academy of Sciences of Ukraine, 61103 Kharkov, Ukraine

<sup>2</sup> Experimental Physics 5, Center for Electronic Correlations and Magnetism, Institute of Physics, University of Augsburg, 86159 Augsburg, Germany

<sup>3</sup> Institute of Applied Physics, Academy of Sciences of Moldova, MD-2028 Chisinau, Republic of Moldova

<sup>4</sup> Physics Department, Moscow State University, 119991 Moscow, Russia

Received 11 April 2011, in final form 29 June 2011

Published 27 July 2011

Online at [stacks.iop.org/JPhysCM/23/325701](http://stacks.iop.org/JPhysCM/23/325701)

## Abstract

The magnetic susceptibility  $\chi$  of  $\text{FeTe}_x$  compounds ( $x \simeq 1.0$ ) was studied under hydrostatic pressure up to 2 kbar at fixed temperatures of 55, 78 and 300 K. Measurements were taken both for polycrystalline and single crystalline samples. At ambient pressure, with decreasing temperature a drastic drop in  $\chi(T)$  was confirmed at  $T \simeq 70$  K, which appears to be closely related to antiferromagnetic ordering. The obtained results have revealed a puzzling growth of susceptibility under pressure, and this effect is enhanced by lowering the temperature. To shed light on the pressure effects in the magnetic properties of  $\text{FeTe}$ , *ab initio* calculations of its volume dependent band structure and the exchange enhanced paramagnetic susceptibility were performed within the local spin density approximation.

## 1. Introduction

The recently discovered superconducting  $\text{FeSe}_{1-x}\text{Te}_x$  compounds [1–5] have attracted extensive attention due to the simplest crystal structure among the new families of iron-based layered compounds exhibiting high temperature superconductivity. This structural simplicity favors experimental and theoretical studies of chemical substitution and high pressure effects, which are aimed at promoting a better understanding of a mechanism of the superconductivity, and also at tuning properties of the novel superconducting materials.

For the  $\text{FeSe}_{1-x}\text{Te}_x$  family, a noticeable increase of the superconducting transition temperature with  $x$  was found, from  $T_c \sim 8$  K at  $x = 0$  to a maximum value of  $\sim 15$  K at  $x \simeq 0.5$ . Additionally, a large enhancement of  $T_c$  up to 35–37 K was observed in  $\text{FeSe}$  under high pressures [6–8]. Similar pressure effects on  $T_c$  have been also reported for  $\text{FeSe}_{0.5}\text{Te}_{0.5}$  [9].

The parent compound  $\text{FeTe}$  is not superconducting but exhibits peculiar magnetic properties. A drastic drop in the temperature dependence of its magnetic susceptibility  $\chi(T)$  with decreasing temperature was observed at  $T \simeq 70$  K, which is related to a first-order structural phase

transition accompanied by the onset of antiferromagnetic (AFM) order [10, 11]. Below the phase transition, the magnetic and crystal structure depends on the amount of excess iron in  $\text{Fe}_{1+x}\text{Te}$  alloys, which possess the same tetragonal crystal structure at room temperature. For nearly stoichiometric  $\text{FeTe}$  compounds, at low temperatures a distorted monoclinic structure and a commensurate in-*ab*-plane AFM ordering were observed [10, 11]. At present, the origin of the strong correlation between the structural and magnetic transitions in  $\text{Fe}_{1+x}\text{Te}$  is not yet clear. On the one hand, it has been argued [10] that the major contribution to the entropy change at the transition(s) can be provided by the AFM ordering. This favors the view that the transition is driven by magnetism. An opposite conclusion was however put forward in [12] based on the analysis of the tetragonal-to-orthorhombic transition taking place in the related  $\text{FeSe}$  compound, which does not exhibit any magnetic order.

Based on the assumption that the suppression of the structural and magnetic transitions stimulates the emergence of superconductivity, attempts have been made to find superconductivity in  $\text{FeTe}$  by applying high pressure [13–15]. However, no trace of superconductivity was detected at

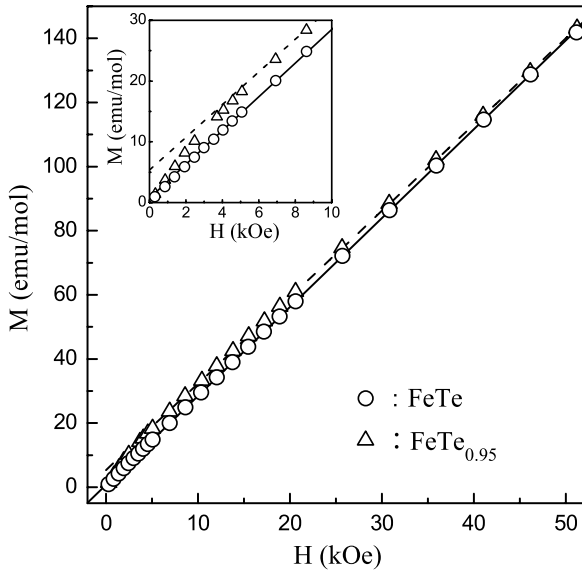


**Figure 1.** Magnetization at  $T = 5$  K of FeTe single crystal ( $H \parallel c$ ) and FeTe<sub>0.95</sub> polycrystalline sample. Inset: the low field data on an expanded scale (see text for details).

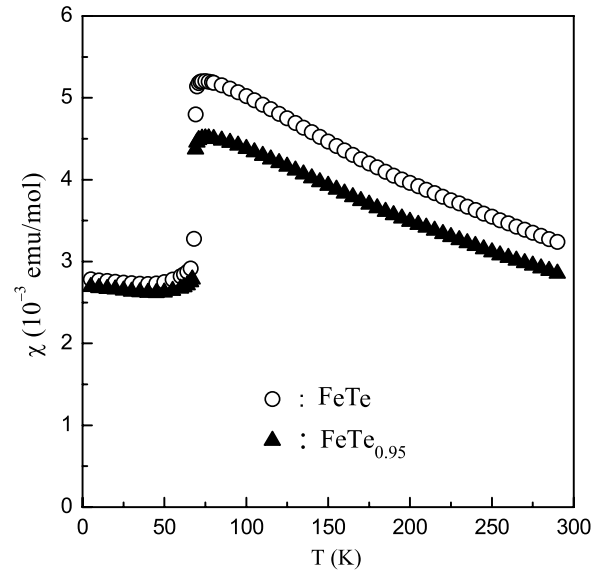


**Figure 2.** Temperature dependence of the magnetic susceptibility for FeTe single crystal and FeTe<sub>0.95</sub> polycrystalline sample.

pressures up to 190 kbar in electrical resistivity measurements, although an anomaly in the resistivity at the structural transition shifted toward lower temperatures with increasing pressure. A similar shift of the magnetic peculiarity with the initial rate of about  $-0.5$  K kbar<sup>-1</sup> was found in the magnetization study under high pressure [15], where a puzzling increase of magnetization with pressure was also observed.

Contrary to the unsuccessful attempts to obtain the superconducting phase under high hydrostatic pressure, superconductivity at about 13 K was detected in FeTe by applying tensile stress conditions in thin films of the compound, which involve an in-plane extension and out-of-plane contraction of the lattice [16]. These experimental data strongly indicate that electronic properties of the FeTe compound are closely correlated with its crystal structure parameters. Further studies of these correlations are expected to shed more light on the nature of magnetism and induced superconductivity in FeTe and on the origin of its magnetic and structural transitions, which are not yet understood [10, 17, 18].

In the present work we report on hydrostatic pressure effects on the magnetic susceptibility of FeTe in its paramagnetic (PM) and AFM states. The obtained results are analyzed using *ab initio* calculations of the volume dependent band structure and the exchange enhanced PM susceptibility of FeTe, which were performed within density functional theory.

## 2. Experimental details and results

Polycrystalline FeTe<sub>0.95</sub> was prepared by conventional solid state synthesis and the FeTe single crystal was grown by a slow-cooling self-flux method [19]. The phase content of the samples was checked by the x-ray diffraction technique.

To check the samples for the presence of ferromagnetic (FM) impurities, which are usually observed in FeSe<sub>1-x</sub>Te<sub>x</sub> compounds and can mask their intrinsic magnetic properties [3, 20, 21], measurements of DC magnetization  $M$  were carried out at  $T = 5$  K with magnetic field  $H$  up to 50 kOe using a superconducting quantum interference device (SQUID) magnetometer. As is seen in figure 1, the  $M(H)$  dependence for the FeTe single crystal (solid line) is quite linear, indicating that the concentration of FM impurities in the sample is negligibly small. For the polycrystalline sample FeTe<sub>0.95</sub>, a nonlinearity of the  $M(H)$  dependence is detected in the low field region (see the inset in figure 1) and a linear behavior prevails at  $H \geq 5$  kOe. The FM saturation moment estimated by linear extrapolation to zero-magnetic field is about  $m_s = 5$  emu mol<sup>-1</sup>.

In figure 2 the temperature dependences of the magnetic susceptibility  $\chi(T)$ , measured in a magnetic field of  $H = 30$  kOe, are shown for the FeTe single crystal ( $H \parallel c$ ) and for polycrystalline FeTe<sub>0.95</sub>. Here the data for FeTe<sub>0.95</sub> were corrected for ferromagnetic impurities by subtracting from the measured magnetic moment  $M(T)$  the saturation moment  $m_s$ , which is assumed to be weakly dependent on  $T$  up to the room temperature [21]. As is seen,  $\chi(T)$  exhibits an anomaly at  $T \simeq 70$ , which is in agreement with the literature data [20, 22–25] and apparently related to the magnetic and structural transitions. In the PM state the observed  $\chi(T)$  behavior is close to the Curie–Weiss law:

$$\chi(T) \simeq C/(T - \Theta), \quad (1)$$

and the values of the PM Curie temperature  $\Theta \simeq -240$  K and Curie constant  $C \simeq 1.7$  K emu mol<sup>-1</sup> ( $\mu_{\text{eff}} \simeq 3.7 \mu_B/\text{Fe}$ ) were estimated for FeTe.

A study of the magnetic susceptibility under helium gas pressure  $P$  up to 2 kbar was performed at fixed temperatures (55, 78 and 300 K) using a pendulum-type magnetometer

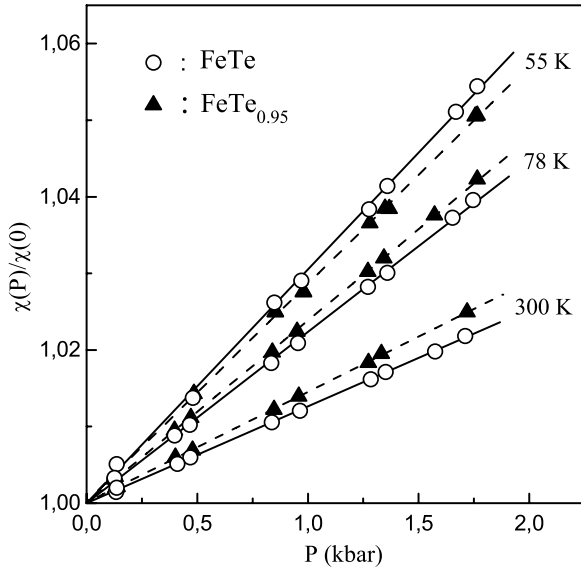


**Figure 3.** Pressure dependence of the magnetic susceptibility, normalized to its value at  $P = 0$ , for single crystalline FeTe (solid line) and polycrystalline FeTe<sub>0.95</sub> (dashed line) compounds at different temperatures.

placed directly in the nonmagnetic pressure cell [26]. The measurements were carried out in a magnetic field  $H = 17$  kOe and their relative errors did not exceed 0.05%. Polycrystalline FeTe<sub>0.95</sub> and single crystalline FeTe studied under pressure had a mass of about 170 and 110 mg, respectively. For the single crystalline FeTe, the magnetic field was applied along the tetragonal  $c$  axis.

The experimental pressure dependences  $\chi(P)$  at different temperatures are shown in figure 3, which demonstrates its size and its linear character. For each temperature and studied sample, the resultant values of pressure derivative  $d \ln \chi / dP$  are given in table 1 together with the corresponding values of  $\chi$  at ambient pressure. Although there is some difference in value of  $\chi$  for the samples, their values of the pressure effect at different temperatures are in reasonable agreement. It should be noted that by using the experimental data on  $d \ln \chi / dP$  for FeTe in the PM state at  $T = 78$  and 300 K, the pressure derivative of the PM Curie temperature was estimated by means of the following equation (which is derived from equation (1)):

$$\frac{d \ln \chi}{dP} = \frac{d \ln C}{dP} + \frac{1}{(T - \Theta)} \frac{d\Theta}{dP} \simeq \frac{\chi}{C} \frac{d\Theta}{dP} \quad (2)$$

to be  $d\Theta/dP \sim 7$  K kbar<sup>-1</sup>. This fact reveals a strong pressure dependence of AFM interaction, which is manifested in the high temperature tetragonal phase of FeTe.

### 3. Computational details and results

To gain further insight into the magnetic properties of FeTe in the normal state, *ab initio* calculations of its electronic structure and exchange enhanced PM susceptibility are performed within density functional theory (DFT) and

**Table 1.** Magnetic susceptibility  $\chi$  (in  $10^{-3}$  emu mol<sup>-1</sup>) and its pressure derivative  $d \ln \chi / dP$  (Mbar<sup>-1</sup>) at different temperatures for polycrystalline FeTe<sub>0.95</sub> and single crystalline FeTe compounds.

		FeTe <sub>0.95</sub>	FeTe
$\chi$	55 K	2.65	2.78
	78 K	4.53	5.19
	300 K	2.82	3.20
$\frac{d \ln \chi}{dP}$	55 K	$28.4 \pm 1.5$	$30 \pm 1.5$
	78 K	$23.8 \pm 1.5$	$22.3 \pm 1.5$
	300 K	$14.4 \pm 0.5$	$12.6 \pm 0.5$

the local spin density approximation (LSDA). At ambient conditions FeTe(Se) possesses the tetragonal PbO-type crystal structure (space group  $P4/nmm$ ), which exhibits strong two-dimensional features. The crystal lattice is composed of alternating triple-layer slabs, which are stacked along the  $c$ -axis. Each iron layer is sandwiched between two nearest-neighbor chalcogen layers, which form edge-shared tetrahedrons around the iron sites. The positions of Te (or Se) sheets are fixed by the internal parameter  $Z_X$ , which represents the height of the chalcogen atoms above the iron square plane. This parameter also determines the chalcogen–Fe bond angles. It was shown [11, 10] that Fe<sub>1+y</sub>Te systems with  $y \leq 0.1$  exhibit a first-order phase transition near 70 K with a tetragonal to monoclinic structural transition. The crystal structure parameters of Fe<sub>1+y</sub>Te compounds were established in a number of works by means of x-ray and neutron diffraction studies [10, 11, 14, 24].

The previous *ab initio* calculations of the electronic structure of the ‘11’-type iron-based chalcogenides were predominantly related to studies of the AFM and SDW (spin-density wave) ordering [27–33]. The aim of this work was mainly to investigate the PM response in an external magnetic field and its volume dependence, as well as to elucidate the nature of the paramagnetism in the parent FeTe compound belonging to the ‘11’ systems. Also, the structural transition from tetragonal to monoclinic structure at 70 K was addressed.

*Ab initio* calculations of the FeTe electronic structure were carried out by employing a full-potential all-electron relativistic linear muffin-tin orbital method (FP-LMTO, code RSPt [34, 35]). No shape approximations were imposed on the charge density or potential, what is especially important for the anisotropic layered crystal structures. The exchange–correlation potential was treated within the LSDA [36] of the DFT.

The calculated basic features of electronic structure for FeTe are in qualitative agreement with the results of earlier calculations (see e.g. [27]). In particular, the tetragonal FeTe compound has the highest density of states at the Fermi level  $N(E_F)$  in the series of FeSe<sub>1-x</sub>Te<sub>x</sub> alloys. With the calculated values of  $N(E_F)$  and the exchange interaction parameter  $I$ , the Stoner criterion  $IN(E_F) \geq 1$  is found to be fulfilled for experimental values of the FeTe unit cell volume  $V_{\text{cell}} \cong 90.9$  Å<sup>3</sup> and internal parameter  $Z_X \cong 0.27$  [10]. This indicates that the PM phase of FeTe compound can be unstable toward an FM state. The electronic structure of FeTe was also calculated as a function of the unit cell volume and parameter

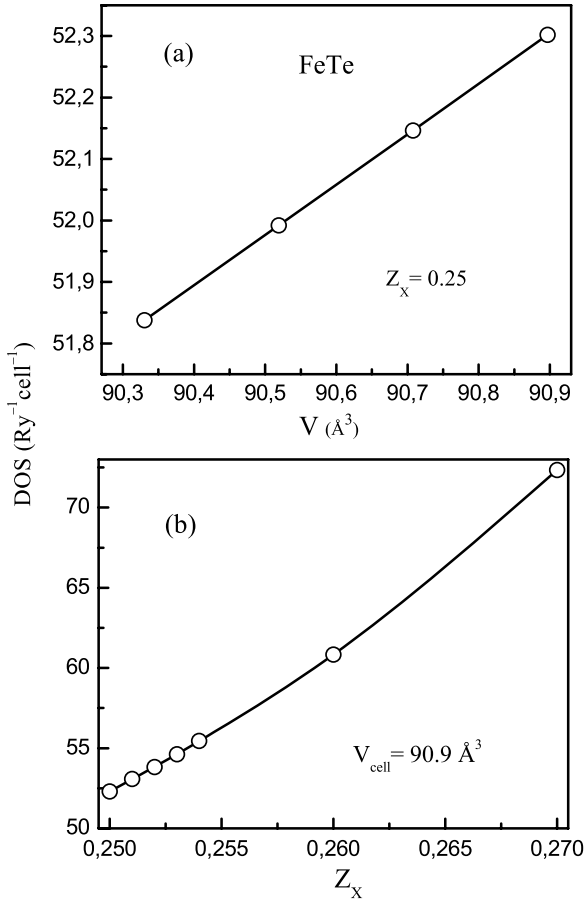


**Figure 4.** Dependences of the density of states at the Fermi level for FeTe on the unit cell volume at fixed values  $c/a = 1.64$  [10] and  $Z_X = 0.25$  (a) and on  $Z_X$  at the fixed experimental unit cell volume (b). The solid line is a guide for the eyes.

$Z_X$ . The results obtained for the density of states at the Fermi level are shown in figure 4 which demonstrates an appreciable dependence of  $N(E_F)$  on the structural parameters, especially on  $Z_X$ .

In order to investigate the observed structural transition from tetragonal to monoclinic structure at 70 K [10, 11] by comparing ground state energies of different structures, the dependences of the total energy on the unit cell volume  $E(V)$  were calculated for both phases (see figure 5). The tetragonal and monoclinic structures were both relaxed in the lattice parameter  $a$ , whereas the lattice parameters  $Z_X$ ,  $c/a$ ,  $b/a$ , and the monoclinic angle  $\beta$  between  $a$  and  $c$  axes, were fixed to their experimental ambient pressure values, which were taken at the phase transition point [10]. The calculated dependences (figure 5) were then fitted with the Murnaghan equation (see e.g. [34]):

$$E(V) = E_{\text{coh}} + \frac{BV_0}{B'} \left( \frac{(V_0/V)^{B'-1}}{B'-1} + \frac{V}{V_0} - \frac{B'}{B'-1} \right). \quad (3)$$

Here  $E_{\text{coh}}$  is the cohesive energy and is treated as an adjustable parameter. Equation (3) is based on the assumption that the pressure derivative  $B'$  of the bulk modulus  $B$  is constant, and it has allowed us to evaluate the equilibrium volumes

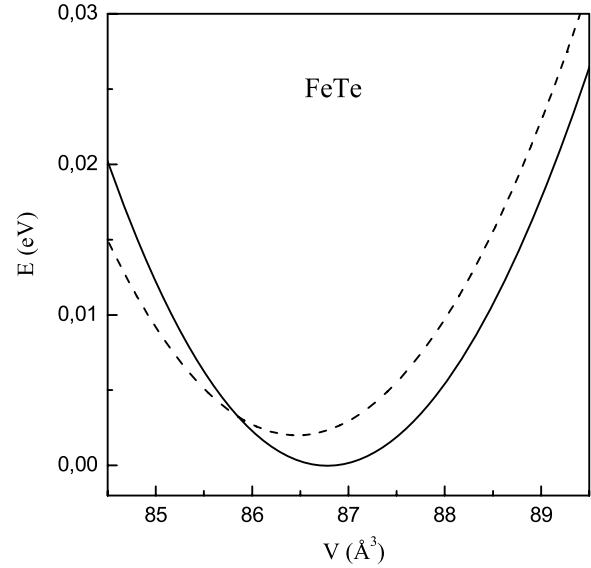


**Figure 5.** Calculated total energy versus volume for FeTe in the monoclinic (solid line) and tetragonal (dashed line) structures. The equilibrium energy of the monoclinic phase is taken to be zero. The lattice parameters  $Z_X$ ,  $c/a$ ,  $b/a$ , and the monoclinic angle  $\beta$  between the  $a$  and  $c$  axes, were fixed to their experimental ambient pressure values at the phase transition point (from [10]).

$V_{\text{tet}} = 86.5 \text{ \AA}^3$  and  $V_{\text{mon}} = 86.8 \text{ \AA}^3$  for the tetragonal and monoclinic structures, correspondingly. Therefore our calculations show that at the point of magnetic phase transition the equilibrium volume of the PM monoclinic phase of FeTe is slightly larger than that of the PM tetragonal phase. It also should be noted that for the PM FeTe the calculated minimum of the total energy for the monoclinic lattice is somewhat lower than for the tetragonal lattice (about  $3 \times 10^{-3}$  eV, see figure 5). This provides some indication that monoclinic distortion can be energetically favorable for FeTe at low temperatures. However, because of the small difference in total energy between the monoclinic and tetragonal structures, the magnetic ordering and lattice dynamical properties should be taken into consideration to shed light on the nature of the simultaneous phase transitions.

Though, according to equation (3), the estimated bulk moduli for the tetragonal and monoclinic case appeared to be rather small,  $B_{\text{tet}} \cong 0.70$  Mbar and  $B_{\text{mon}} \cong 0.80$  Mbar, they are substantially larger than the reported experimental values for the related FeSe compound,  $B_{\text{exp}} \cong 0.30$  Mbar [6, 37, 38]. This is probably related to the well known overbonding tendency of the LSDA approach, and a better agreement between the theoretical and experiment bulk moduli presumably can be obtained by optimization of the lattice parameters and internal ionic coordinates within the generalized gradient approximation (GGA); see [34]. However, for further analysis of the pressure effect on  $\chi$  it seems more reliable to use the experimental value of  $B$ .

To estimate the paramagnetic susceptibility of FeTe and its pressure dependence, FP-LMTO-LSDA calculations of the field-induced spin and orbital (Van Vleck) magnetic moments were carried out within the approach described in [39].

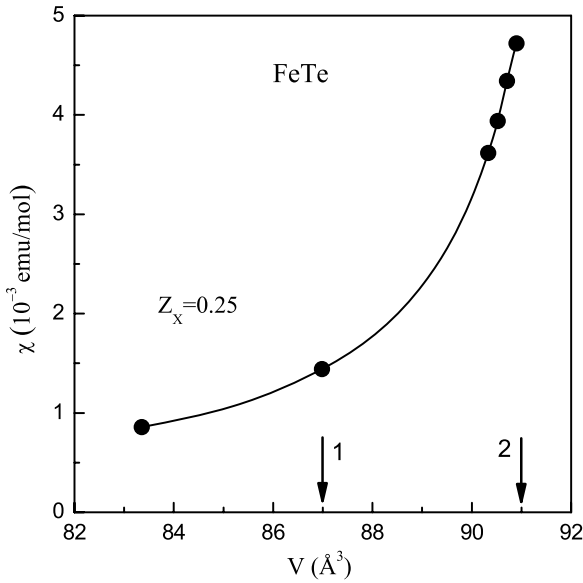


**Figure 6.** Calculated PM susceptibility of FeTe versus the unit cell volume.  $Z_X$  is taken to be 0.25, and the  $c/a$  ratio is fixed to the experimental ambient pressure value (1.64, [10]). The arrows indicate the theoretical (1) and experimental (2) volume values. The solid line is a guide for the eye.

All relativistic effects, including spin–orbit coupling, were incorporated, and the effect of an external magnetic field  $\mathbf{H}$  was taken into account self-consistently at each iteration by means of the Zeeman term:

$$\mathcal{H}_Z = \mu_B \mathbf{H} \cdot (2\hat{\mathbf{s}} + \hat{\mathbf{l}}), \quad (4)$$

which was incorporated in the original FP-LMTO Hamiltonian. Here  $\mathbf{H}$  is the external magnetic field,  $\mu_B$  the Bohr magneton,  $\hat{\mathbf{s}}$  and  $\hat{\mathbf{l}}$  the spin and orbital angular momentum operators, respectively. When the field-induced spin and orbital magnetic moments are calculated, the corresponding volume magnetization can be evaluated, and the ratio between magnetization and field strength provides the susceptibility.

The results of the field-induced calculations also indicate the instability of the PM state of FeTe toward an FM state, which was predicted above within the Stoner approach for the experimental lattice parameters. The convergence of the self-consistent field-induced LSDA calculations was actually achieved only for reduced values of the structural parameters, the cell volume and  $Z_X$ . In figure 6 the calculated total magnetic susceptibility of FeTe is presented versus the unit cell volume. This volume dependence was derived from the field-induced magnetic moments, which were calculated in the external field of 10 T providing the internal parameter  $Z_X$  is reduced by about 10% of its experimental value. The calculated dependence of the magnetic susceptibility on  $Z_X$  at the fixed LSDA optimized ground state volume is shown in figure 7.

As seen from figures 6 and 7, the calculated PM susceptibility for FeTe, as well as the density of states at the Fermi level (figure 4), both reveal a strong sensitivity to the unit cell volume and, especially, to the  $Z_X$  parameter. The

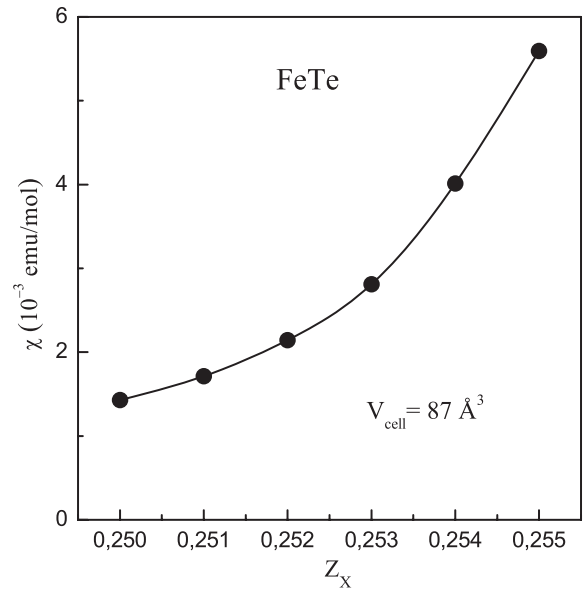


**Figure 7.** Calculated PM susceptibility of FeTe as a function of  $Z_X$  for the LSDA optimized ( $87 \text{ \AA}^3$ ) unit cell volume. The  $c/a$  ratio is fixed to the experimental ambient pressure value (1.64, [10]). The solid line is a guide for the eye.

calculated PM susceptibilities, being of the same order as the experimental ones, should be considered as a crude estimate which can be used to establish a trend for the effects of the structural parameters on  $\chi$ .

#### 4. Discussion

In order to elucidate the main mechanism of the experimentally observed strong increase of the magnetic susceptibility of FeTe under pressure, we have attempted to analyze the pressure effect in terms of the corresponding change of the volume and  $Z_X$  parameters by using the relation

$$\frac{d \ln \chi}{dP} = \frac{\partial \ln \chi}{\partial \ln V} \times \frac{d \ln V}{dP} + \frac{\partial \ln \chi}{\partial Z_X} \times \frac{dZ_X}{dP}. \quad (5)$$

The required values of the partial volume and  $Z_X$  derivatives of  $\chi$  can be estimated from the results presented in figures 6 and 7, and were found to be approximately  $\partial \ln \chi / \partial \ln V \sim 40$  and  $\partial \ln \chi / \partial Z_X \sim 350$  for the values of  $\chi \sim (3-4) \times 10^{-3} \text{ emu mol}^{-1}$ , which are close to the experimental data. Then the first term in equation (5) has a large negative value of about  $-120 \text{ Mbar}^{-1}$ , provided we take for compressibility of FeTe the value  $d \ln V / dP \simeq -3 \text{ Mbar}^{-1}$ , which is reported for the related FeSe compound [6, 37, 38]. When compared to the experimental positive value of the pressure effect (see table 1), this term does not appear to be the dominating one. Hence one can assume that a change of  $Z_X$  under pressure can play a dominant role in equation (5), also taking into account the calculated strong dependence of susceptibility on  $Z_X$  (see figure 7). In the absence of data on  $dZ_X/dP$  for FeTe, we can fit the experimental pressure effect  $d \ln \chi / dP \sim 20 \text{ Mbar}^{-1}$  for FeTe in the PM state by setting  $dZ_X/dP = 0.40 \text{ Mbar}^{-1}$ , which provides a large positive value of the second term in

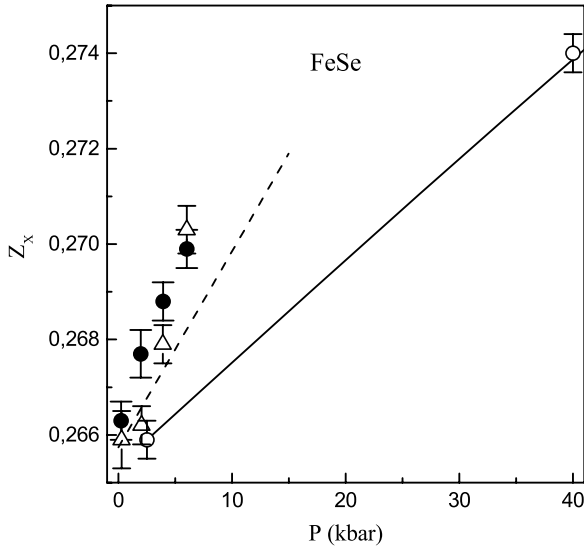


**Figure 8.** Experimental data on pressure dependence of  $Z_X$  in FeSe for the tetragonal phase at  $T = 190$  K (●) and the orthorhombic phase at  $T = 50$  K (△) from [37] and for the orthorhombic phase at  $T = 16$  K (○) from [8]. The dashed line corresponds to  $Z_X(P)$  dependence which provides the best fit of equation (5) to the experimental data for FeTe.

equation (5),  $\partial \ln \chi / \partial Z_X \times dZ_X/dP \simeq 140 \text{ Mbar}^{-1}$ . Actually, the above choice of the  $dZ_X/dP$  derivative is consistent with the available experimental data on the pressure dependence of the  $Z_X$  parameter for the related FeSe compound, as is seen in figure 8.

It should be noted that the observed large positive pressure effect on  $\chi$  was reasonably explained above relying on the results of *ab initio* calculations for the PM spin susceptibility and the density of electronic states (figures 4, 6 and 7). Thus the obtained description of the experimental data within equation (5) is based on the assumed itinerant nature of the magnetic susceptibility in FeTe. It may be suggested that the positive pressure effect on  $\chi$  is caused by a peculiar behavior of the density of states at the Fermi level under pressure, presumably due to its apparent sensitivity to the structural parameters, particularly to the internal parameter  $Z_X$ .

The measured pressure derivative of the magnetic susceptibility  $d \ln \chi / dP$  can be used to evaluate the spontaneous volume change in FeTe due to the AFM ordering,  $\Delta V / V \equiv \omega_m$ , which is related to the mean-square magnetic moment  $M^2(T)$  (see [40] and references therein):

$$\omega_m(T) = \frac{C}{B} M^2(T). \quad (6)$$

Here  $B$  is the bulk modulus,  $C$  the magnetoelastic coupling constant. The latter can be determined in the context of a band theory of magnetism within the phenomenological relation [40, 41]

$$\frac{C}{B} = -\frac{1}{2\chi V_m} \frac{d \ln \chi}{dP}, \quad (7)$$

where  $\chi$  and  $V_m$  are the molar susceptibility and volume, respectively. By using in equation (7) the experimental values

of  $\chi$  and  $d \ln \chi / dP$  from table 1 and  $V_m \simeq 27.3 \text{ cm}^3$  [18], we estimated the magnetoelastic constant for FeTe in the AFM state to be

$$\frac{C}{B} = -(1.8 \pm 0.3) \times 10^{-10} (\text{emu/mol})^{-2}. \quad (8)$$

Using equation (6) and substituting the experimental value of the magnetic moment ( $M(0) \sim 2 \mu_B/\text{Fe}$  [10, 11]) and the above  $C/B$  value, provides the volume change in FeTe at the AFM transition to be  $\omega_m(0) \sim -0.02$ .

At first glance, it would seem that this estimate is qualitatively consistent with the experimental value  $\omega_m(0) \simeq -0.01$ , which results from the thermal expansion measurements for  $\text{Fe}_{1.06}\text{Te}$  [42]. However, the validity of this comparison is questionable because of the coexistence of the AFM ordering with the structural phase transition. Moreover, the thermal expansion data of [42] contradict the results of structural studies that show no detectable change in volume during the transition [10, 11, 18]. Up to now, there is no experimental evidence of the magnetovolume effect  $\omega_m(0)$ , which, in fact, can be hidden due to a close interplay of the AFM ordering and the structural phase transition. Based upon the results of our *ab initio* calculations we can suggest that the low temperature monoclinic phase might have a larger volume in the absence of magnetic ordering. When FeTe undergoes a transition to the AFM state, this transition is presumably accompanied by volume contraction of the monoclinic phase. This would explain the absence of detectable change in the volume during the AFM transition [10, 11, 18]. Then, due to the application of pressure, a structural transition from the monoclinic phase with a larger volume to the tetragonal phase with a smaller volume would be expected to be shifted to lower temperatures. This prediction is in accordance with the experimental behavior of the peculiarity around 70 K under pressure.

## 5. Conclusions

For polycrystalline and single crystalline  $\text{FeTe}_x$  compounds with  $x \simeq 1$  the precision measurements of magnetic susceptibility were carried out under hydrostatic pressure at temperatures both above and below the transition point. The strong positive pressure effect on  $\chi$  was revealed which qualitatively does not depend on the magnetic state of the sample. The estimated spontaneous change in volume at the AFM ordering is shown to be about 2% and presumably hidden from direct detection because of the close interplay of the magnetic and structural phase transitions.

*Ab initio* FP-LMTO-LSDA calculations of the electronic structure and PM contributions to the susceptibility of FeTe revealed that this system is close to magnetic instability with dominating enhanced spin paramagnetism. The calculated values of the density of states at the Fermi level and PM susceptibility exhibit a strong dependence on the structural parameters, such as the unit cell volume  $V_{\text{cell}}$  and especially the height  $Z_X$  of chalcogen species from the Fe plane. With appropriate values of these parameters a reasonable agreement between calculated and experimental values of  $\chi$

at ambient pressure could be obtained. Based on the results of calculations, the puzzling experimental pressure effect on  $\chi$  for FeTe can be represented as a sum of two large in magnitude and competing contributions, resulted from the pressure dependence of the structural parameters  $V_{\text{cell}}$  and  $Z_X$ , the latter determining the dominant positive contribution.

The obtained results point out that the itinerant magnetism approach is relevant to describe the PM phase of FeTe, as well as of the related FeSe compound [21]. However, due to the apparently more localized nature of the 3d states, these results have to be thoroughly verified by other methods, and compared with experimental data. Specifically, more rigorous calculations of  $\chi$  are required for FeTe, which would take into account disordered local magnetic moments above the magnetic transition temperature. In particular, the recently employed *ab initio* DLM (disordered local moments) approach [33, 43] seems very promising to shed more light on the nature of magnetism in the FeTe compound.

## Acknowledgments

This work has been supported by the Russian–Ukrainian RFBR–NASU project 43-02-10 and 10-02-90409, and by NASU Young Scientists Grant 16-2011. The support of DFG via SPP1458 is also acknowledged.

## References

- [1] Hsu F-C *et al* 2008 *Proc. Natl Acad. Sci. USA* **38** 14262
- [2] McQueen T M *et al* 2009 *Phys. Rev. B* **79** 014522
- [3] Pomjakushina E, Conder K, Pomjakushin V, Bendele M and Khasanov R 2009 *Phys. Rev. B* **80** 024517
- [4] Yeh K-W *et al* 2008 *Europhys. Lett.* **84** 37002
- [5] Mizuguchi Y and Takano Y 2010 *J. Phys. Soc. Japan* **79** 102001
- [6] Braithwaite D, Salce B, Lapertot G, Bourdarot F, Marin C, Aoki D and Hanfland M 2009 *J. Phys.: Condens. Matter* **21** 232202
- [7] Medvedev S *et al* 2009 *Nature Mater.* **8** 630
- [8] Margadonna S, Takabayashi Y, Ohishi Y, Mizuguchi Y, Takano Y, Kagayama T, Nakagawa T, Takata M and Prassides K 2009 *Phys. Rev. B* **80** 064506
- [9] Tsoi G, Stemshorn A K, Vohra Y K, Wu P M, Hsu F C, Huang Y L, Wu M K, Yeh K W and Weir S T 2009 *J. Phys.: Condens. Matter* **21** 232201
- [10] Li S *et al* 2009 *Phys. Rev. B* **79** 054503
- [11] Bao W *et al* 2009 *Phys. Rev. Lett.* **102** 247001
- [12] McQueen T M, Williams A J, Stephens P W, Tao J, Zhu Y, Ksenofontov V, Casper F, Felser C and Cava R J 2009 *Phys. Rev. Lett.* **103** 057002
- [13] Takahashi H, Okada H, Takahashi H, Mizuguchi Y and Takano Y 2010 *J. Phys.: Conf. Series* **200** 012196
- [14] Mizuguchi Y, Tomioka F, Tsuda S, Yamaguchi T and Takano Y 2009 *Physica C* **469** 1027
- [15] Okada H, Takahashi H, Mizuguchi Y, Takano Y and Takahashi H 2009 *J. Phys. Soc. Japan* **78** 083709
- [16] Han Y, Li W Y, Cao L X, Wang X Y, Xu B, Zhao B R, Guo Y Q and Yang J L 2010 *Phys. Rev. Lett.* **104** 017003
- [17] Moon C-Y and Choi H J 2010 *Phys. Rev. Lett.* **104** 057003
- [18] Martinelli A, Palenzona A, Tropeano M, Ferdeghini C, Putti M, Cimberle M R, Nguyen T D, Affronte M and Ritter C 2010 *Phys. Rev. B* **81** 094115
- [19] Tsurkan V, Deisenhofer J, Günther A, Kant Ch, Krug von Nidda H-A, Schrettle F and Loidl A 2011 *Eur. Phys. J. B* **79** 289
- [20] Chen G F, Chen Z G, Dong J, Hu W Z, Li G, Zhang X D, Zheng P, Luo J L and Wang N L 2009 *Phys. Rev. B* **79** 140509(R)
- [21] Fedorchenko A V *et al* 2011 *Low Temp. Phys.* **37** 83
- [22] Iikubo S, Fujita M, Niitaka S and Takagi H 2009 *J. Phys. Soc. Japan* **78** 103704
- [23] Yang J, Matsui M, Kawa M, Ohta H, Michioka C, Dong C, Wang H, Yuan H, Fang M and Yoshimura K 2010 *J. Phys. Soc. Japan* **79** 074704
- [24] Sales B C, Sefat A S, McGuire M A, Jin R Y, Mandrus D and Mozharivskiy Y 2009 *Phys. Rev. B* **79** 094521
- [25] Viennois R, Giannini E, van der Marel D and Černý R 2010 *J. Solid State Chem.* **183** 769
- [26] Panfilov A S 1992 *Phys. Tech. High Pressures* **2** 61 (in Russian)
- [27] Subedi A, Zhang L, Singh D J and Du M H 2008 *Phys. Rev. B* **78** 134514
- [28] Zhang L, Singh D J and Du M-H 2009 *Phys. Rev. B* **79** 012506
- [29] Ma F, Ji W, Hu J, Lu Z-Y and Xiang T 2009 *Phys. Rev. Lett.* **102** 177003
- [30] Lee K-W, Pardo V and Pickett W E 2008 *Phys. Rev. B* **78** 174502
- [31] Han M-J and Savrasov S Y 2009 *Phys. Rev. Lett.* **103** 067001
- [32] Ding Y, Wang Y and Ni J 2009 *Solid State Commun.* **149** 505
- [33] Chadov S, Scharf D, Fecher G H, Felser C, Zhang L and Singh D J 2010 *Phys. Rev. B* **81** 104523
- [34] Wills J M, Eriksson O, Alouani M and Price D L 2000 *Electronic Structure and Physical Properties of Solids: The Uses of the LMTO Method* ed H Dreysse (Berlin: Springer) p 148  
Alouani M and Wills J M 2000 *Electronic Structure and Physical Properties of Solids: The Uses of the LMTO Method* (Berlin: Springer) p 168  
Eriksson O and Wills J M 2000 *Electronic Structure and Physical Properties of Solids: The Uses of the LMTO Method* (Berlin: Springer) p 247
- [35] Wills J M, Alouani M, Andersson P, Delin A, Eriksson O and Grechnev A 2010 *Full-Potential Electronic Structure Method* (Berlin: Springer)
- [36] von Barth U and Hedin L 1972 *J. Phys. C: Solid State Phys.* **5** 1629
- [37] Millican J N, Phelan D, Thomas E L, Leao J B and Carpenter E 2009 *Solid State Commun.* **149** 707
- [38] Garbarino G, Sow A, Lejay P, Sulpice A, Toulemonde P, Mezouar M and Nunez-Regueiro M 2009 *Europhys. Lett.* **86** 27001
- [39] Grechnev G E, Ahuja R and Eriksson O 2003 *Phys. Rev. B* **68** 64414
- [40] Fawcett E, Kaiser A B and White G K 1986 *Phys. Rev. B* **34** 6248
- [41] Kortekaas T F M and Franse J J M 1976 *J. Phys. F: Met. Phys.* **6** 1161
- [42] Budko S L, Canfield P C, Sefat A S, Sales B C, McGuire M A and Mandrus D 2009 *Phys. Rev. B* **80** 134523
- [43] Ruban A V, Khmelevskiy S, Mohn P and Johansson B 2007 *Phys. Rev. B* **75** 054402